Chiral 3,3'-(1,2-ethanediyl)-bis[2-(3,4-dimethoxyphenyl)-4-thiazolidinones] with anti-inflammatory activity. Part II: Evaluation of COX-2 selectivity and modelling

ARTICLE *in* BIOORGANIC & MEDICINAL CHEMISTRY · MARCH 2003

Impact Factor: 2.79 · DOI: 10.1016/S0968-0896(02)00518-7 · Source: PubMed

Pergamon

SCIENCE DIRECT®

Bioorganic & Medicinal Chemistry 11 (2003) 999–1006

BIOORGANIC & MEDICINAL CHEMISTRY

Chiral 3,3′-(1,2-Ethanediyl)-bis[2-(3,4-dimethoxyphenyl)-4-thiazolidinones] with Anti-Inflammatory Activity. Part 11: Evaluation of COX-2 Selectivity and Modelling†

M. G. Vigorita,[a,*] R. Ottanà,[a] F. Monforte,[a] R. Maccari,[a] M. T. Monforte,[b] A. Trovato,[b] M. F. Taviano,[b] N. Miceli,[b] G. De Luca,[c] S. Alcaro[d] and F. Ortuso[d]

[a]*Dipartimento Farmaco-chimico, Facoltà di Farmacia Università di Messina, Viale SS. Annunziata, 98168 Messina, Italy*
[b]*Dipartmento Farmaco-biologico, Facoltà di Farmacia Università di Messina, Viale SS. Annunziata, 98168 Messina, Italy*
[c]*Istituto di Scienze Biochimiche e Biochimica Clinica, Facoltà di Medicina e Chirurgia Università di Messina, Policlinico Universitario 'G. Martino', V. Cons. Valeria, 98124 Messina, Italy*
[d]*Dipartimento di Scienze Farmacobiologiche, Università di Catanzaro 'Magna Græcia', Roccelletta di Borgia, Catanzaro, Italy*

Received 14 June 2002; accepted 9 October 2002

Abstract—Anti-inflammatory/analgesic 3,3′-(1,2-ethanediyl)-bis[2-(3,4-dimethoxyphenyl)-4-thiazolidinones] **1**, obtained as racemic mixtures (**a**) and mesoforms (**b**), have two equivalent stereogenic centres (C-2 and C-2′) and exist as *RR*, *SS* and *RS* isomers. The enantioseparation of **1a** provided the single enantiomers that displayed different in vitro cyclooxygenase-1/cyclooxygenase-2 selectivity ratios. In particular the dextrorotatory compound is a highly selective COX-2 inhibitor and the levorotatory one is moderately selective. Instead, *RS-meso* isomer (**1b**) exhibited similar levels of inhibitory activity on both COX isozymes. The diastereo- and enantioselectivity has been explained by molecular modelling of *RR*, *SS* and *RS* compounds into COX-1 and COX-2 binding sites. Theoretical results indicated *SS* > *RS* > *RR* affinity order towards COX-2 isoenzyme, in agreement with in vitro and previous in vivo pharmacological results.

Introduction

In the last decade, the discovery and characterisation of cyclooxygenase-2 (COX-2) isoform has greatly improved the understanding of the inflammatory process.[1–4] As a consequence, several classes of selective COX-2 inhibitors have been developed.[5–7] Two diarylheterocycles, celecoxib and rofecoxib, have been recently marketed in many countries as potent COX-2 selective inhibitors.[8,9] Such novel NSAIDs are indicated as able to circumvent gastrointestinal (GI) adverse effects associated with traditional therapy, because they typically inhibit inducible COX-2 isoform while they spare 'housekeeping' COX-1 with its benefits.[10]

In fact, COX-1 and COX-2 serve different physiological and pathophysiological functions: COX-1 is the constitutive isoform, mainly responsible for the synthesis of cytoprotective prostaglandins in the gastrointestinal tract; COX-2, the inducible and short-lived isoform, is overexpressed in inflammatory cells in response to endotoxins, cytokines and mitogens.[6,8]

Interesting anti-inflammatory/analgesic/antipyretic agents derived from the 3,3′-(1,2-ethanediyl)-bis[2-aryl/heteroaryl-4-thiazolidinone] chiral system (Fig. 1) have long been investigated in our laboratories.[11–16]

Such compounds with two equivalent stereogenic centres (C-2 and C-2′) were obtained and pharmacologically explored as 2*R*,2′*R*/2*S*,2′*S* racemic mixture (**a**) and 2*R* 2′*S-meso* isomers (**b**). These latter generally displayed better in vivo anti-inflammatory (AI), analgesic and antipyretic activities than corresponding racemates[15,16] which, as expected, showed great variability of responses because

*Corresponding author. Tel.: +39-090-676-6469; fax: +39-090-355613; e-mail: vigorita@pharma.unime.it
†A Preliminary account of this work was presented at First Magna Græcia Medicinal Chemistry Workshop on New Perspectives in Drug Research, Copanello, CZ, Italy, 10–13 June 2001.

0968-0896/03/$ - see front matter © 2002 Elsevier Science Ltd. All rights reserved.
PII: S0968-0896(02)00518-7

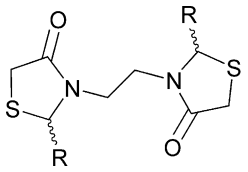

R = Ar, Het
rac. 2R,2'R/2S,2'S (**a**)
2R,2'S-*meso* (**b**)

Figure 1. General formula of 3,3′-(1,2-ethanediyl)-bis[2-aryl/heteroaryl-4-thiazolidinones] (BIS 2*C).

of the possible different contribution of the single enantiomers. The nature of substituents on stereogenic carbons were also found to influence the onset and the level of AI effects: methoxyphenyl substitution when R = Ar, and pyridine groups when R = Het, proved to be the most favourable among the numerous substitutions investigated.[12,16] Interestingly, all bisthiazolidinones so far tested exhibited a high degree of gastrointestinal (GI) tolerance even at high doses, independently of stereochemistry and nature of substituents.[11,12,14–16]

In the unsuccessful attempt to find a rationalisation for the apparent relationship between stereochemistry and AI activity, in the past we carried out an extensive conformational analysis, starting from X-ray diffractrometric data of some aryl/heteroaryl BIS 2*C,[14] in solution and by quantum-chemical methods.[13] Taken together, these studies had shown that bisthiazolidinones are highly flexible molecules. In particular, 2*R*,2′*S*-*meso* isomers exhibit in solid phase the antiperiplanar conformation of the ethylendiamine chain while in solution they exist as rapidly interconverting mixtures of three rotamers (two *gauche* and one *trans*) in approximately equal proportions. The modeling carried out by semiempirical computer program AM1 indicated that the free molecule has two *gauche* rotamers (N–C–C–N dihedral angle about 70°) with comparable stability and a slightly less stable antiperiplanar conformation. 2*R*,2′*R*/2S,2′*S* racemic mixtures, instead, prefer syn-clinal conformations and this preference persists in $CDCl_3$ solution and in the free molecules.[13]

We have recently focused our interest on BIS 2*C bearing methoxyphenyl substituents at 2,2′ positions and in particular on 2*R*,2′*R*/2*S*,2′*S* (**1a**) and 2*R*,2′*S*-*meso* (**1b**) 3,4-dimethoxyphenyl substituted derivatives endowed with excellent in vivo AI profiles.[16] In particular, in the classical anti-inflammatory carrageenin-induced paw edema test, *meso*form **1b**, which was assumed as lead compound, exhibited antiedemigen effects ranging from 58 to 63% at 100 mg/kg dose over the 3 h from carrageenin injection, while racemic mixture **1a** provided 76% inhibition of paw edema only after the second hour. Both compounds were free of GI side effects. Although we are aware of the complexity of the inflammatory process, [17] these observations led to the hypothesis that the *RR*, *SS* and *RS* isomers could be preferential diastereo/enantioselective COX-2 inhibitors.

Therefore, for further insight, we have planned the theoretical and experimental studies the results of which are the object of this note. Namely, (i) a docking procedure could contribute to understand the differences between the interaction modes of *RR*, *SS* and *RS* isomers with both COX isoforms, taking advantage of the available structures of the COX-1 and COX-2 co-crystallized complexes with known NSAIDs;[18,19] (ii) the human whole blood COX-1/COX-2 selectivity assay[20] performed on the three stereoisomers could provide experimental evidence to rationalize the different in vivo AI profiles of BIS 2*C under investigation. This information would allow a targeted optimization of anti-inflammatory agents BIS 2*C.

Results and Discussion

Computational study

The conformational search detailed in the Experimental has been applied to model *RR*, *SS* and *RS* stereoisomers into COX-1 and COX-2 binding sites. The selected models, namely ICXE and 6COX from PDB files relative to complexes of flurbiprofen with ovine COX-1[18] and SC-558 with murine COX-2,[19] respectively, represented the best choice in terms of resolution among deposited structures. Only aminoacid residues found in the 10 Å radium from the ligand have been considered. The in situ molecular dynamics have been carried out, as detailed in the experimentals, to understand the structural origin of the selectivity more deeply. The results, expressed as enzyme/inhibitor [E/L] interaction energy and ligand internal energy, are collected in Table 1, which also contains two geometrical descriptors of the *RR*, *SS* and *RS* minimum conformations docked in both binding sites.

Energetic data indicate that *SS* enantiomer has the highest COX-2 affinity as shown by its interaction

Table 1. Geometrical descriptors,[a] E/L interaction and ligand internal energies

Isomer	Isozyme	N–C–C–N dihedral angle (°)	Ar/Ar distance (Å)	Enzyme/ligand interaction energy (kcal/mol)	Ligand internal energy (kcal/mol)
RR	COX-1	−163.15	5.706	3.73	41.88
	COX-2	−77.01	4.478	−3.31	10.66
SS	COX-1	−134.85	6.124[b]	14.74	53.01
	COX-2	−154.59	7.443	−47.15	12.06
RS	COX-1	−83.80	7.824	−37.93	25.62
	COX-2	59.37	4.603	−46.88	28.93

[a]In global minimum conformations within the enzyme clefts.
[b]The conformation is folded because the phenyl A is spatially close to the thiazolidinone moiety B.

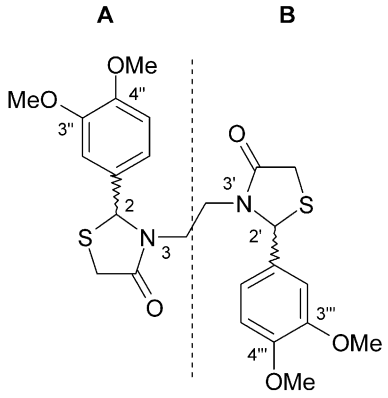

Figure 2. Numbering scheme of 3,3′-(1,2-ethanediyl)-bis[2-(3,4-dimethoxyphenyl)-4-thiazolidinone].

energy (−47.15 kcal/mol) in the preferred extended conformation; it also has a more favourable internal energy (12.06 kcal/mol) if compared to that measured into COX-1 catalytic site.

RR enantiomer has low affinity for both enzymes, as shown by its E/L interaction energies (3.73 and −3.31 kcal/mol, respectively). The preference toward COX-2 enzyme is due to the folded conformation with quite different internal energy (10.66 vs 41.88 kcal/mol into COX-1 site).

Meso compound can interact with both isozymes, by assuming folded conformations: higher affinity toward COX-2, however, is demonstrated by the relevant difference in the E/L interaction energies close to 10 kcal/mol.

As reported by several Authors, the COX catalytic site consists of a long narrow hydrophobic channel with a 'hairpin bend' at the end.[2,6,21] The main aminoacidic residues critical for NSAIDs interaction are Arg120 in the mouth of the channel, near to its constriction, Tyr385, Tyr355, Tyr348 and Ser530. The non-conserved residue at position 523, which is isoleucine in COX-1 and valine in COX-2, is considered the most important for ligand selective recognition. In fact, by inducing a Tyr 355 conformational change, the smaller valine side chain gives access to an additional side pocket, into which the sulphonamide or sulphone groups of celecoxib and COX-2 selective congeners can insert themselves.[2,6d,19,21] Different mutagenesis experiments indicated that this single substitution is able to convert COX-1 isozyme into an enzyme which can be inhibited by COX-2 selective inhibitors.[22]

The different features of COX catalytic sites, together with the flexibility and the 2,2′ carbons configuration of our ligands, appear to be responsible for the different interaction modes of *RR*, *SS* and *RS* stereomers with the isozymes.

The *RR* isomer, owing to its stereochemistry, cannot occupy the additional pocket more accessible by the Val523Ile substitution in COX-2 isoform. The stabilization of E/L complex appears to be mainly influenced by two H-bonds between Arg120 and the 3″ (moiety A) and 4‴ (moiety B) methoxylic oxygens (Figs. 2 and 3a).

In COX-1 binding site, *RR* isomer undergoes a conformational change and N–C–C–N dihedral angle varies from −77.01° (COX-2) to −163.15° (COX-1) (Table 1). In consequence, moiety A rotates while moiety B remains in the same position as in COX-2 site with its H bond with Arg120 (Fig. 3b); the ligand internal energy is greatly enhanced and the steric hindrance of Ile523 also makes the E/L complex highly destabilized.

In contrast, the *SS* enantiomer can deeply penetrate into the larger COX-2 catalytic site (Fig. 4a) by assuming an extended conformation, favoured by the configuration *S* of both stereogenic centers, that offers a larger surface to the protein interactions. Differently from *RR* isomer, no H-bond between Arg120 and methoxylic

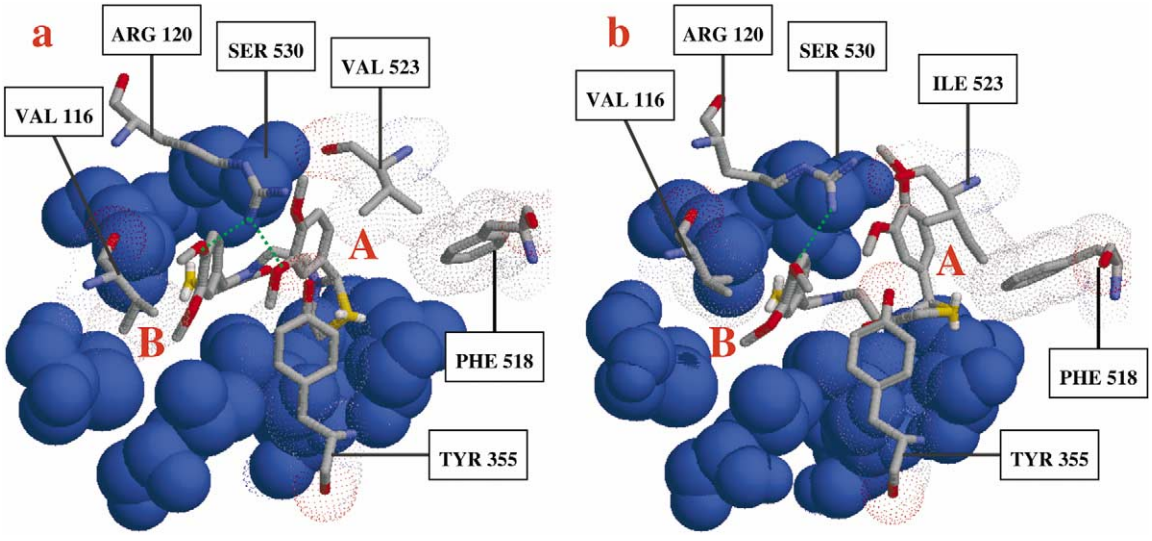

Figure 3. Entrance view of the *RR* compound into the COX-2 (a) and COX-1 (b) binding sites. A and B labels refer to Figure 2. Dotted lines show the intermolecular H-bond network favouring the COX-2 recognition. A detailed list of E·L interaction is reported in Table 2. *In all figures, for clarity, Tyr385 and Tyr348 residues are undisplayed since they are in the most internal position of both binding sites.*

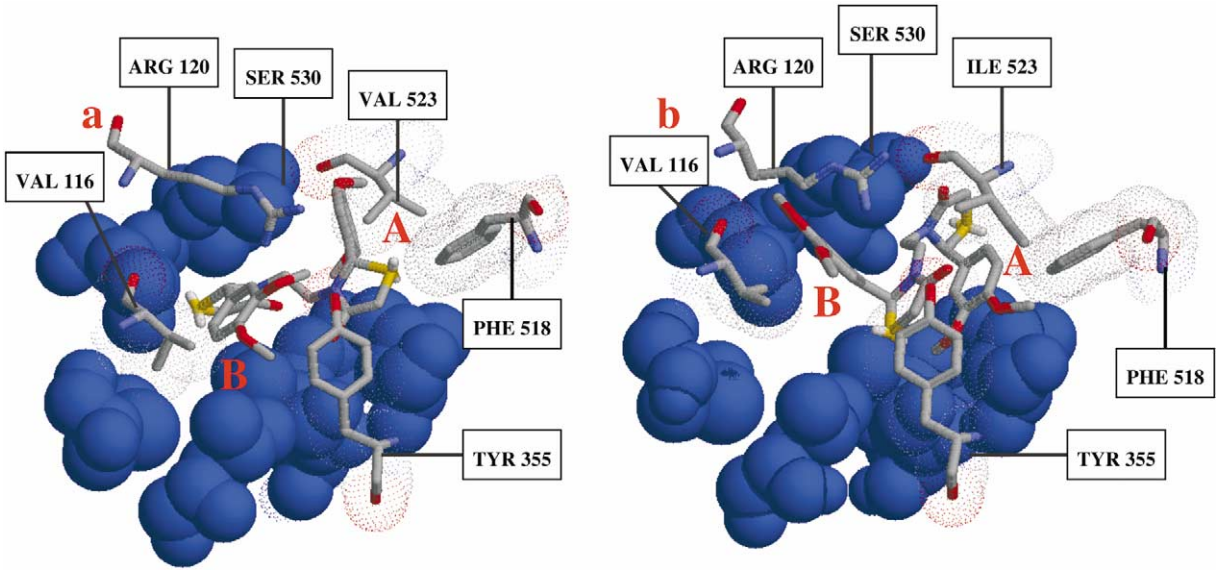

Figure 4. Entrance view of the *SS* compound into the COX-2 (a) and COX-1 (b) binding sites. A and B labels refer to Figure 2. No intermolecular hydrogen bond network was detected. The steric effect of the different residue 523 is crucial for the distinctive recognition of this compound between two isoenzymes. A detailed list of E·L interaction is reported in Table 2.

oxygens is detectable, but there are electrostatic and VdW interactions with this and other residues (Val116, Ser530 and Tyr385).

In COX-1 binding site (Fig. 4b), the *SS* ligand is forced to assume a folded minimum conformation (N–C–C–N angle of −134.85°). The heterocyclic moiety A is located within the hydrophobic pocket delimited by Ile523, Tyr355 and Phe518. The 3- and 4-methoxy groups on ring B interact with Arg120 by means of electrostatic and VdW forces, not by H-bonds which are not sterically possible. Minor Van der Waals interactions are established with other aminoacidic residues such as the Val116.

In conclusion, the *SS* enantiomer is able to take advantage of the larger volume available in COX-2 in which it can assume a stable minimum conformation characterized by favourable internal energy and by the lowest E/L interaction energy (−47.15 kcal/mol). In addition, it can occupy a deeper position than in COX-1 binding site where it remains more towards the exterior (Fig. 4b).

The conformation of the *meso* isomer into COX-2 cavity is characterized by a N–C–C–N dihedral angle equal to 59.37°. Both moieties, A containing *R* carbon and B containing *S* carbon, are anchored by H-bonds to Arg120 (Fig. 5a). In addition, the methoxyphenyl group on *R* carbon that hydrophobically interacts with Val523 and the adjacent thiazolidinone moiety fill the lateral pocket delimited by Val523, Phe518, whereas electrostatic interactions are established with Ser530 and, more weakly, with other residues. The complex E/L results greatly stabilized, although the ligand internal energy is moderately high (Table 1).

Also in COX-1 cavity the *meso* isomer assumes a conformation able to establish an H-bond between Arg120 and carbonylic sp_2 oxygen of moiety A, that also interacts with Ser530 with electrostatic and VdW forces. Instead, the thiazolidinone ring bearing *S* carbon (moiety B) gives hydrophobic interactions with Ile523 and its sp_2 oxygen electrostatically interacts with the OH of Tyr355 (Fig. 5b). In addition, the aromatic ring of moiety A is able to establish strong hydrophobic interactions with Val349 and Leu531 placed above and below its plane respectively. The Van der Waals contact analysis reveals that the steric contribution is determinant for the definition of *meso* isomer folding properties within the COX-1 site. The ligand is sterically forced in a more external position with respect to the COX-2 enzyme cleft.

The energy analysis assesses, for the *RS* isomer, negative E/L interaction energies in both enzyme sites with a moderate preference for COX-2 isoform.

In Table 2, a detailed list of interactions between each stereoisomer and the isoenzymes is reported.

COX-1/COX-2 selective inhibition in vitro assay

Before measuring the COX-1/COX-2 inhibitory activity of the three isomers, the resolution of racemic mixture **1a** has been effected by means of an enantioselective HPLC procedure. In particular the former eluate provided the levorotatory antipode ($[\alpha]_D^{25} = -52.8$) and the latter provided the dextrorotatory one ($[\alpha]_D^{25} = +53$). The three isomers, however, have been submitted to the human whole blood assay following Patrignani and Patrono's method. This assay allows the assessment of in vitro COX-1/COX-2 selectivity using whole blood from healthy volunteers. The measurement of PGE_2 production in response to LPS added to heparinized blood samples reflects the time-dependent induction of COX-2 in circulating monocytes. The parallel measurement of TBX_2 production during whole blood clotting is used as an index of platelet COX-1 activity.[20]

Table 2. Summary of the main interactions between the *RR*, *SS* and *RS* stereoisomers and the enzymes in the global minimum energy conformations

Stereisomer	Ligand-moiety[a]	COX-2	Type[b]	Ligand-moiety[a]	COX-1	Type[b]
RR	3-MeO *A*	Arg120	HB	4-MeO *B*	Arg120	HB
	4-MeO *B*					
	4 C=O *B*	Tyr385	EL	4 C=O *B*	Ser530 Tyr385 Tyr348	EL
	S *B*	Ser530	EL	4-MeO *B*	Val116 Tyr355	EL
	Ar *B*	Val116 Leu531	HP	Ar *B*	Leu531	HP
		Leu359 Met113				
		Val349 Ala527				
	Thiazolidinone *B*	Val349	HP	Thiazolidinone *B*	Val349	HP
	Ar *A*	Val523 Ala527	HP	3-MeO *B*	Val116 Leu531 Met113 Leu359	HP
	Thiazolidinone *A*	Leu352 Val349	HP	4-MeO *A*	Ala527 Ile523 Met525 Pro528	HP
				3-MeO *A*	Ile523	HP
				Ar *A*	Ile523	HP
SS	3-MeO *B*	Arg120	EL	3-MeO *B*	Arg120	EL
	3-MeO *A*	Tyr385	EL	4 C=O *B*	Gly526	EL
	4 C=O *A*	Tyr385	EL	S *B*	Ser353	EL
	3-N *B*	Ser530	EL	4 C=O *A*	Tyr355	EL
	4-MeO *B*	Val116 Val349 Leu359	HP	S *A*	Tyr348 Tyr385	EL
	Ar *B*	Ala527 Leu531 Val349	HP	3-MeO *B*	Val116	HP
	Thiazolidinone *B*	Val344 Val349 Leu535	HP	4-MeO *B*	Leu531 Pro528	HP
	Thiazolidinone *A*	Val523 Leu352	HP	Ar *B*	Leu531 Ala527	HP
	Ar *A*	Val523 Leu384	HP	Thiazolidinone *B*	Val349 Leu359	HP
	4-MeO *A*	Tyr385	HP	Thiazolidinone *A*	Met522 Trp387	HP
				Ar *A*	Leu352 Ile523	HP
				3-MeO *A*	Val349	HP
RS	3-MeO *B* 3-MeO *A*	Arg120	HB	4 C=O *A*	Arg120	HB
	4-MeO *B*	Leu531 Val116 Met113 Leu359	HP	Ar *A* 4-MeO *A* 3-MeO *A*	Val116 Met113 Leu357	HP
	3-MeO *B*	Val116	HP	Thiazolidinone *A*	Leu531 Val116 Ala527 Val349	HP
	Ar *B*	Leu531 Ala527 Val349	HP	4 C=O *B*	Tyr355	EL
	S *B*	Ser530	EL	Thiazolidinone *B*	Leu352 Phe518 Ile523 Ala527	HP
	4 C=O *B*	Tyr348	EL	4-MeO *B* 3-MeO *B*	Tyr348 Tyr385 Ser530	EL
	Thiazolidinone *A*	Leu352 Phe518 Val523	HP	4-MeO *B*	Val349 Val344	HP
	4 C=O *A*	Tyr355	EL	3-MeO *B*	Phe381 Leu384 Trp387	HP
	4-MeO *A*	Ala527 Val523	HP	Ar *A*	Ala527 Met522 Leu352 Val349	HP
	3-MeO *A*	Tyr355	HP			
	Ar *A*	Val523	HP			

[a]A/B specification refers to Figure 2.
[b]HB, hydrogen bond; EL, electrostatic; HP, hydrophobic.

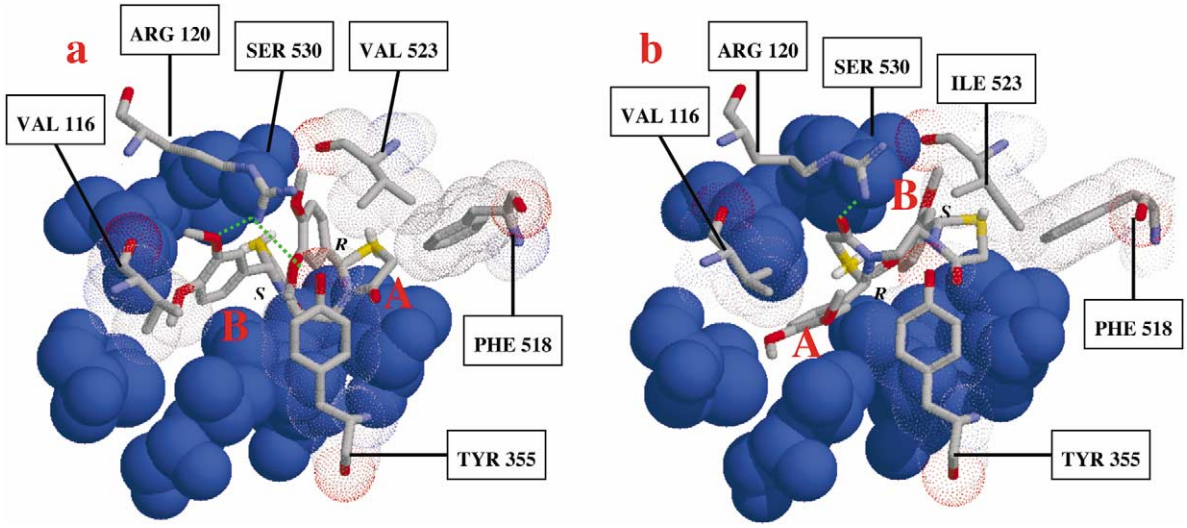

Figure 5. Entrance view of the *meso* compound into the COX-2 (a) and COX-1 (b) binding sites. A and B labels refer to Figure 2 and *R*/*S* to the stereogenic centers. Dotted lines show the intermolecular H-bond network favouring the COX-2 recognition. A detailed list of E·L interaction is reported in Table 2.

Table 3. COX-1 and COX-2 inhibition (IC_{50}, μM) and selectivity ratios on human whole blood assay

Compd	COX-1	COX-2	COX-1/COX-2 selectivity ratio[a]
(+) **1a**[b]	>100	0.316	>316.45
(−) **1a**[c]	>100	4.68	>21.36
meso **1b**	2.44	1.62	1.51
Nimesulide	26.9	1.51	17.8
Rofecoxib[d]			410.0

[a]IC_{50} (μM) media values from multiple samples; SE is in the range of 20%.
[b]$[\alpha]_D^{25} = +53$ in ethanol.
[c]$[\alpha]_D^{25} = -52.8$ in ethanol.
[d]From ref 20b.

The results of this assay, expressed as IC_{50} (μM), are reported in Table 3. Nimesulide in our hand confirmed to be a moderately selective COX-2 inhibitor as indicated by the selectivity ratio of 17.8 that agrees with data reported in literature.[20c] *RS* isomer **1b** proves to be a non-selective COX inhibitor, whereas the levorotatory isomer is a relatively selective COX-2 inhibitor (S.R. >21). The dextrorotatory enantiomer, instead, shows high COX-2 inhibitory potency with a selectivity ratio approximating that of rofecoxib, determined by the same assay;[20b] thus it can be considered the 'eutomer' in this series.

The in vitro results appear to be in agreement with those already observed in vivo:[16] in fact, the AI activity shown by racemic mixture **1a** (76% of carrageenin edema inhibtion at the third h) is originated by the sum of (+) 'eutomer' and (−) 'distomer' antiedemigen effects. The delayed onset of inhibitory activity is a typical feature of COX-2 selective NSAIDs.[3,7,23] In contrast, the origin of the constant levels of AI effects over the three hours shown by *RS* isomer **1b** agrees with the lack of COX selectivity.

Conclusions

In this paper, we described the in vitro COX-1/COX-2 selectivity assay used to ascertain the COX-2 preference of 3,3′-(1,2-ethanediyl)-bis[2-(3,4-dimethoxyphenyl)-4-thiazolidinone] isomers suggested by previously obtained in vivo results.[16] It was found that, among the tested diatereoisomers, the most selective COX-2 inhibitor is the dextrorotatory enantiomer which can be considered the 'eutomer', whereas *RS-meso* isomer is not selective. The levorotatory 'distomer' places itself in an intermediate level of COX-2 preference.

The configurational assignments, however, remains an open question at least until a greater amount of each enantiomer will give the possibility of having suitable crystals for X-ray analysis.

Considering the intrinsic molecular mechanics approximation in evaluation of the intermolecular energies, our docking results revealed the COX-2 selectivity order *SS*> *RS*> *RR*, which was also shown by other methoxyphenyl congeners.[24,25] The docking study indicated that recognition process is mainly driven by the configurations of 2,2′ carbons along with methoxyphenyl substitutents on them. Into the larger COX-2 binding site all stereoisomers can find the necessary space to fit themselves and adjust their conformation, although none of them can deeply penetrate in the 'critical' side pocket more accessible by non conserved Val523 residue.

The methoxy substituents were confirmed to be favourable since they support the diastereo- and enantioselective recognition process.[24,25]

Therefore, the main SARs pointed out during the course of our research on aryl/heteroaryl bisthiazolidinones could find convincing explanations. In particular, (a) the typical GI safety feature can be correlated with their preferential COX-2 inhibition; (b) the variability of AI response in *RR*/*SS* mixtures might be due to the sum of qualitatively and quantitatively different contributions of eutomer and distomer in each racemate; (c) the *RS-meso* AI profiles, seemingly better than those of the corresponding racemates, could be thoroughly explained by the presence of both stereogenic centers; in fact, the molecules become each time able to make a choice of the best recognition process into COX catalytic sites.

In our opinion, this research system could afford a method to design more selective COX-2 ligands in the bisthiazolidinone class, that will be synthesised, enantioseparated and pharmacologically assayed only if it is worthwhile.

Experimental

Chemistry

Experimental procedures to obtain **1a** and **1b** and their characterization were reported in refs 15 and 16.

Enantioseparation. Racemate 2*R*,2′*S*/2*S*,2′*R* (**1a**) was resolved by analytical scale HPLC.[26] The HPLC system consisted of a Shimadzu Model class VP5 chromatograph. The mobile phase was HPLC-grade *n*-hexane/2-propanol 3/7 mixture. As stationary phase a Chiralcel OD column (cellulose bis-3,5-dimethylphenylcarbamate) was used. The separation was carried out at 25 °C. The former eluated fractions provide the levorotatory enantiomer with $[\alpha]_D^{25} = -52.8$ (ethanol), while the latter fractions give the dextrorotatory one with $[\alpha]_D^{25} = +53$ (ethanol) (Perkin–Elmer 341 Polarimeter).

Computational methods

To study the interaction between the three isomers and the COX-1 and COX-2 enzymes, the crystallographic models of such macromolecules deposited into the PDB were considered. The selection of the models 1CQE [18] and 6COX,[19] relative respectively to COX-1 and COX-2 co-crystals with non covalent ligands (known NSAIDs) was carried out considering the lowest resolution factor with respect to other available PDB structures.

A preliminary analysis of the ligand binding modes into the two selected PDB models allowed us to identify the aminoacid residues responsible of the recognition selectivity with COX-1/COX-2 inhibitors. We considered the aminoacids within 10 Å from the crystallographic position of each ligand in the original PDB structures. Both COX-1 and COX-2 cyclooxygenase portions of the catalytic sites are delimited by the Tyr385 residue that hinders the heme group from the ligand position. Therefore, we excluded the porphyrine moiety from our models. Following this procedure, we obtained our reduced model taking in account 73 and 87 aminoacids respectively for COX-1 and COX-2.

Starting geometries of the enzyme–inhibitor [E·I] complexes were generated by placing an energy minimized conformation of each ligand into the binding site.

We have performed a preliminary ligand conformational search by a 1000-step Monte Carlo simulation, followed by multiminimization in GB/SA water. Each ligand global minimum was manually docked into the enzyme clefts and submitted to a protein constrained energy minimization in GB/SA water creating our starting geometries of the enzyme–inhibitor [E·I]. These complexes were submitted to 100 ps of molecular stochastic dynamic mix-mode simulations[27] at 300 K using Amber* force field[28] as implemented in MacroModel package.[29] In these calculations the atom coordinates of the enzymes were constrained applying the standard force constant of 100 kJ/mol. No constrain was applied to the inhibitor. In order to relax the internal degrees of freedom of the ligand, the conformations generated by the previous step were minimized with the same force field and constrains.

Finally the enzyme–ligand interaction energies were calculated with the MOLINE package [30] using the same molecular mechanics parameters of the AMBER* force field. The internal energies of the ligand were extrapolated from the conformations assumed by the inhibitor in the global minima obtained after the mix-mode and enzyme-constrained simulations.

Pharmacology

(+)**1a**, (−) **1a**, and **1b** were tested at four different concentrations (ranging from 10^{-5} to 10^{-8} M) for selectivity against COX-1/COX-2 isoenzymes by means of the human whole blood assay performed following Patrignani's procedure.[20]

Whole blood was drawn from donors when they had not taken any NSAIDs during the 2 weeks preceding the study. One-millilitre aliquots of whole blood were immediately transferred into glass tubes and allowed to clot at 37 °C for 60 min. Serum was separated by centrifugation (10 min at 2000 rpm) and kept at −80 °C until assayed for TXB_2. Whole blood TXB_2 production was measured by EIA as a reflection of maximally stimulated cyclooxygenase activity of platelet COX-1 by endogenously formed thrombin.

One-millilitre aliquots of whole blood samples from the same donors, containing 10 IU of sodium heparin were incubated both in the absence and in the presence of LPS (10 μg/mL) for 24 h at 37 °C. The contribution of platelet COX-1 was suppressed by adding aspirin (10 μg/mL) in vitro at time 0. Plasma was separated by centrifugation (10 min at 2000 rpm) and kept at −80 °C until assayed for PGE_2. PGE_2 production by LPS-stimulated monocytes was measured by EIA.

Tested compounds were dissolved in ethanol and 30 μL aliquot of each solution was pipetted directly into test tubes at fixed concentration from 10^{-8} to 10^{-5} M. The solvent was evaporated and 1-mL aliquots of heparinized whole blood were added. The effects of *meso*form **1b**, (+) **1a** and (−) **1a** enantiomers on COX-1 activity were evaluated by incubating each compound at four different concentrations with multiple whole blood samples that were allowed to clot at 37 °C for 60 min. The effects of the compounds on COX-2 activity were studied by incubating the compounds at four different concentrations with multiple heparinized whole blood samples in the presence of LPS (10 μg/mL) for 24 h.

Acknowledgements

This work was financially supported by the Ministero dell'Università e della Ricerca Scientifica e Tecnologica (MURST-Rome), and the Assessorato Beni Culturali e Ambientali della Pubblica Istruzione — Regione Siciliana (Italy) (D.A n. 1175 30/12/1998; Cap. 77504).

References and Notes

1. Vane, J. R. *Nature* **1994**, *367*, 215.
2. Hawkey, C. J. *Lancet* **1999**, *353*, 307.
3. Jouzeau, J.; Terlain, B.; Abid, A.; Nedelec, E.; Netter, P. *Drugs* **1997**, *53*, 563.
4. Bakhle, Y. S. *Drugs Today* **1999**, *35*, 237.
5. Cannon, G. W. *Drugs Today* **1999**, *35*, 487.
6. (a) Kalgutkar, A. S.; Marnet, A. B.; Crews, B. C.; Remmel, R. P.; Marnet, L. J. *J. Med. Chem.* **2000**, *43*, 2860 and references cited therein. (b) Bayly, C. I.; Black, W. C.; Leger, S.; Ouimet, N.; Ouellet, M.; Percival, M. D. *Bioorg. Med. Chem. Lett.* **1999**, *9*, 307. (c) Wilkerson, W. W.; Copeland, R. A.; Covington, M.; Trzaskos, J. M. *J. Med. Chem.* **1995**, *38*, 3895. (d) Amgad, G.; Habeeb, P. N.; Praveen, Rao; Knaus, Edward E. *J. Med. Chem.* **2001**, *44*, 2921. (e) Amgad, G.; Habeeb, P. N.; Rao, P.; Knaus, E. E. *J. Med. Chem.* **2001**, *44*, 3039.
7. Marnet, L. J.; Kalgutkar, A. S. *TiPS* **1999**, *20*, 465.
8. (a) Penning, T. D.; Talley, J. J; Bertenshaw, S. R.; Carter, J. S.; Collins, P. W.; Docter, S.; Graneto, M. J.; Lee, L. F.; Malecha, J. W.; MiYashiro, J. M.; Rogers, R. S.; Rogier, D. J.; Yu, S. S.; Andreson, G. D.; Burton, E. G.; Cogburn, J. N.; Gregory, S. A.; Koboldt, C. M.; Perkins, W. E.; Seibert, K.; Veenhuizen, A. W.; Zhang, Y. Y.; Isakson, P. C. *J. Med. Chem.* **1997**, *40*, 1347. (b) *Drugs Future*, **1997**, *22*, 711
9. (a) Scott, L. J.; Lamb, H. M. *Drugs* **1999**, *58*, 499. (b) Prasit, P.; Wang, Z.; Brideau, C.; Chan, C.-C.; Charleson, S.; Cromlish, W.; Ethier, D.; Evans, J. F.; Ford-Hutchinson, A. W.; Gauthier, J. Y.; Gordon, R.; Guay, J.; Gresser, M.; Kargman, S.; Kennedy, B.; Leblanc, Y.; Leger, S.; Mancini, J.; O'Neill, G. P.; Ouellet, M.; Percival, M. D.; Perrier, H.;

Riendeau, D.; Rodger, I.; Tagari, P.; Therien, M.; Vickers, P.; Wong, E.; Xu, L.-J.; Young, R. N.; Zamboni, R.; Boyce, S.; Rupniak, N.; Forrest, M.; Visco, D.; Patrick, D. *Bioorg. Med. Chem. Lett*. **1999**, *9*, 1773.
10. Emery, P. *Drugs Today* **1999**, *35*, 267.
11. Vigorita, M. G.; Previtera, T.; Basile, M.; Fenech, G.; Costa De Pasquale, R.; Occhiuto, F.; Circosta, C. *Il Farmaco* **1988**, *4*, 373.
12. Previtera, T.; Vigorita, M. G.; Basile, M.; Fenech, G.; Trovato, A.; Occhiuto, F.; Monforte, M. T.; Barbera, R. *Eur. J. Med. Chem*. **1990**, *2*, 569.
13. Previtera, T.; Vigorita, M. G.; Basile, M.; Orsini, F.; Benetollo, F.; Bombieri, G. *Eur. J. Med. Chem*. **1994**, *29*, 317.
14. Benetollo, F.; Bombieri, G.; Del Pra, A.; Basile, M.; Previtera, T.; Vigorita, M. G. *J. Cryst. Spectr. Res*. **1991**, *21*, 113.
15. Vigorita, M. G.; Previtera, T.; Ottanà, R.; Grillone, I.; Monforte, F.; Monforte, M. T.; Trovato, A.; Rossitto, A. *Il Farmaco* **1997**, *52*, 43.
16. Vigorita, M. G.; Ottanà, R.; Monforte, F.; Maccari, R.; Trovato, A.; Monforte, M. T.; Taviano, M. F. *Bioorg. Med. Chem. Lett*. **2001**, *11*, 2791.
17. (a) Higgs, G. A.; Higgs, A.; Moncada, S. The Arachidonic Acid Cascade. In *Comprehensive Medicinal Chemistry*; Hansch, C., Ed.; Pergamon, Oxford: 1990, Vol. 2; p 147. (b) Crow, J. P.; Beckmann, J. S. *Adv. Pharmacol*. **1995**, *34*, 17.
18. Picot, D.; Loll, P. J.; Garavito, R. M. *Nature* **1994**, *367*, 243.
19. Kurumbail, R. G.; Stevens, A. M.; Gierse, J. K.; McDonald, J. J.; Stegeman, R. A.; Pak, J. Y.; Gildehaus, D.; Miyashiro, J. M.; Penning, T. D.; Seibert, K.; Isakson, P. C.; Stallings, W. C. *Nature* **1996**, *384*, 644.
20. (a) Patrignani, P.; Panara, M. R.; Greco, A.; Fusco, O.; Natoli, C.; Iacobelli, S.; Cipollone, F.; Ganci, A.; Creminon, C.; Maclouf, J.; Patrono, C. *J. Pharmacol. Exp. Ther*. **1994**, *271*, 1705. (b) Patrignani, P. *Toxicol. Lett*. **2000**, *112-113*, 493. (c) Patrono, C.; Ciabattoni, G.; Pinca, E.; Pugliese, F.; Castrucci, G.; De Salvo, A.; Satta, M. A.; Peskar, B. A. *Thromb. Res*. **1980**, *17*, 317.
21. Filizola, M.; Perez, J. J.; Palomer, A.; Mauleon, D. *J. Mol. Graph. Model*. **1997**, *15*, 290.
22. Gierse, J.; McDonald, J.; Hauser, S.; Rangwala, S.; Seibert, K. *J. Biol. Chem*. **1996**, *271*, 15810.
23. Copeland, R. A.; Williams, J. M.; Giannaras, J.; Nurnberg, S.; Covington, M.; Pinto, D.; Pick, S.; Trzaskos, J. M. *Proc. Natl. Acad. Sci. U.S.A*. **1994**, *91*, 11202.
24. Ottaná, R.; Mazzon, E.; Dugo, L.; Monforte, F.; Maccari, R.; Sautebin, L.; De Luca, G.; Vigorita, M. G.; Alcaro, S.; Ortuso, F.; Caputi, A. P.; Cuzzocrea, S. *Eur. J. Pharmacol*. **2002**, *448*, 71.
25. Ottaná, R.; Monforte, F.; Alcaro, S.; De Luca, G.; Maccari, R.; Ortuso, F.; Vigorita, M. G. First Magna Græcia Medicinal Chemistry Workshop on New Perspectives in Drug Research, Copanello, CZ, 10–13 June 2001.
26. Caccamese, S.; Principato, G.; Ottanà, R.; Previtera, T.; Zappalà, C. *J. Chromatogr. A* **1995**, *694*, 355.
27. Guarnieri, F.; Still, W. C. *J. Comput. Chem*. **1994**, *15*, 1302.
28. McDonald, D. Q.; Still, W. C. *Tetrahedron Lett*. **1992**, *33*, 7743.
29. MacroModel version 5.5 for SGI Mohamadi, F.; Richards, N. G. J.; Guida, W. C.; Liskamp, R.; Lipton, M.; Caufield, C.; Chang, G.; Hendrickson, T.; Still, W. C. *J. Comput. Chem*. **1990**, *11*, 440.
30. Alcaro, S.; Gasparrini, F.; Incani, O.; Mecucci, S.; Misiti, D.; Pierini, M.; Villani, C. A. *J. Comput. Chem*. **2000**, *21*, 515.